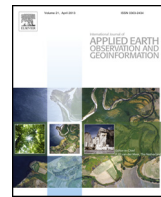




Contents lists available at ScienceDirect

# International Journal of Applied Earth Observation and Geoinformation

journal homepage: [www.elsevier.com/locate/jag](http://www.elsevier.com/locate/jag)



## Remote sensing of vegetation cover dynamics and resilience across southern Africa



A. Harris<sup>a,\*</sup>, A.S. Carr<sup>b</sup>, J. Dash<sup>c</sup>

<sup>a</sup> Geography, School of Environment and Development, University of Manchester, Manchester M13 9PL, United Kingdom

<sup>b</sup> Department of Geography, University of Leicester, Leicester LE1 7RH, United Kingdom

<sup>c</sup> Geography and Environment, University of Southampton, Southampton SO17 1BJ, United Kingdom

### ARTICLE INFO

#### Article history:

Received 22 March 2013

Accepted 21 November 2013

#### Keywords:

Remote sensing

Trend analysis

Land degradation

NDVI

AVHRR

Africa

### ABSTRACT

Southern Africa supports a significant portion of the world's floral biodiversity but predicted changes in climate are likely to cause adverse impacts on the region's ecosystems and biodiversity. Knowledge regarding the resilience of vegetation cover is important for understanding the potential impact of anthropic or climatic change. The length of time vegetation cover takes to recover from disturbances can provide an indication of ecosystem resilience. We investigated spatial and temporal patterns in the persistence of vegetation cover across southern Africa (1982–2006) and used persistence probability plots to estimate decay times of NDVI trends as a means to characterise the potential resilience of key southern African biomes. Patterns of positive and negative NDVI trend persistence were spatially coherent, indicating collective dynamic behaviour of vegetation cover. Persistence probability plots indicated differences in resilience between biomes. Mean recovery times from negative NDVI trends were shorter than for positive trends in the Savanna and Nama Karoo, whereas the Succulent Karoo exhibited the shortest mean lifetime for positive NDVI trends and one of the longest mean lifetimes for negative trend survival, implying potentially slow recovery from environmental disturbance. The results show the potential of satellite-time series data for monitoring vegetation cover resilience in semi-arid regions.

© 2013 Elsevier B.V. All rights reserved.

## 1. Introduction

Changes in vegetation cover as a consequence of predicted anthropogenic climate change, or other land-use related pressures (e.g. fires, overgrazing and land abandonment) may have a substantial effect upon the world's ecosystems (e.g.; Midgley & Thuiller, 2011; Schaphoff et al., 2006; Scholze et al., 2006). Like much of the African continent, southern Africa is considered highly vulnerable to future climatic change (Fauchereau et al., 2003; Thomas et al., 2005; IPCC, 2007). An increased frequency and intensity of extreme climatic events, such as droughts, is likely to cause major changes in vegetation cover, with attendant socio-economic implications (Reynolds et al., 2007). There is a growing research impetus to identify ways to detect early signs of climate change and identify regions and ecosystems of high vulnerability (Midgley & Thuiller, 2011).

Vegetation responses to an environmental perturbation depend upon the frequency and magnitude of the disturbance, the relationships between the perturbing factors (e.g. temperature, precipitation, land use; Hutyra et al., 2005) and the resilience of

the ecosystem concerned. Quantification of the persistence and resilience of vegetation cover, across various spatial and temporal scales, will facilitate a greater understanding of both baseline vegetation dynamics and the responses of ecosystems to human activities or natural stresses (Gunderson, 2000).

Different definitions of resilience exist with the ecological literature (Gunderson, 2000), although the most common definition considers ecological systems to exist close to a stable steady-state (Holling, 1996). Therefore, resilience can be defined as the ability of a system to return to a stable steady-state following a perturbation. The time taken for the vegetation to recover can be used as one measure of vegetation resilience (Tilman & Downing, 1994; Ives, 1995; Mittelbach et al., 1995). The vegetation recovery time is inversely proportional to the level of resilience (Wissel, 1984). Under quasi-stable conditions, healthy vegetation is expected to be more resilient, whereas environmental stresses can reduce resilience and cause persistent decreases in vegetation activity (Lanfredi et al., 2004; Simonello et al., 2008). Despite its simplicity, this definition of resilience is often used for large-scale studies of vegetation dynamics, particularly those relying on remotely sensed data where vegetation cover is often characterised as either being present or absent.

Spatial coverage and the availability of time-series data render remote sensing systems an ideal tool with which to consider such large-scale vegetation dynamics. The NOAA-AVHRR (National

\* Corresponding author. Tel.: +44 023 8059 9224.

E-mail addresses: [angela.harris@manchester.ac.uk](mailto:angela.harris@manchester.ac.uk) (A. Harris), [asc18@leicester.ac.uk](mailto:asc18@leicester.ac.uk) (A.S. Carr), [j.dash@soton.ac.uk](mailto:j.dash@soton.ac.uk) (J. Dash).

Oceanic and Atmospheric Administration Advanced Very High Resolution Radiometer) sensors currently provide the most comprehensive time-series of satellite data for monitoring regional-scale changes on the Earth's surface. Specifically, the Normalised Difference Vegetation Index (NDVI), which derived from red and near infrared reflectance bands of the AVHRR sensor, is an established satellite vegetation index commonly used as a surrogate for vegetation biomass, cover and vitality (e.g. Tucker, 1979; Myneni et al., 1997). AVHRR data have previously been used to study trends in greenness in arid and semi-arid areas, both globally (e.g. Nemani et al., 2003; Xiao and Moody, 2005; Beck et al., 2011; de Jong et al., 2011; Fensholt et al., 2012) and at a regional level (e.g. Hellden and Otrup, 2008; Huber and Fensholt, 2011).

The aim of this paper is to characterise vegetation dynamics and resilience across southern Africa between 1982 and 2006 using AVHRR data, and to assess the potential of this approach for monitoring the vulnerability of key African biomes to environmental change. We followed a method developed by Lanfredi et al. (2004), which provides an estimation of the persistence probability of vegetation cover. From this, timescales of vegetation cover recovery can be deduced and related to vegetation resilience. Using AVHRR-NDVI data, we investigate spatial patterns in the persistence of vegetation cover at the regional and biome scale across Botswana, South Africa, Namibia, Swaziland and Lesotho and use the estimated decay times of NDVI trends as a means of characterising biome specific resilience. In doing so, this study will be the first to apply this specific technique to arid and semi-arid regions and biomes such as the Succulent Karoo of western South Africa. The range of biomes across the study area, which are characterised by different plant physiologies and structural characteristics, in conjunction with significant climatic gradients and varying degrees of climatic variability, also make this a useful region in which to test this approach to resilience analysis.

## 2. Study area

The study area encompasses five countries and a diversity of environmental conditions. Seven major biomes are recognised across this region, five of which (Fynbos, Succulent Karoo, Nama Karoo, Grassland and Savanna) are the focus here. These biomes are largely differentiated on the basis of dominant plant life form, which in turn reflects marked gradients in rainfall seasonality and summer aridity across the sub-continent (Rutherford, 1997; Dlamini, 2011; Wessels et al., 2011). Substrate (soil) has little influence on biome-scale categorisations (Rutherford, 1997), although some exceptions do exist (e.g. Succulent Karoo/Fynbos). Mean annual rainfall is extremely variable across the study area, ranging from c. 800 mm per annum in south east South Africa, to <50 mm per annum in hyper-arid Namibia. Isohyets, which are orientated in a broadly east–west manner in more tropical latitudes, become increasingly north–south orientated in central South Africa and the south-western parts of the subcontinent, which reflects the increasing significance of the mid-latitude anticyclones relative to the ITCZ (Intertropical Convergence Zone) in driving atmospheric stability and rainfall patterns (Lindesay, 1998).

There is little conclusive evidence for long-term increases or decreases in southern African precipitation throughout the twentieth century (Richard et al., 2001; Hoffman et al., 2009). Some evidence has been reported for a drying trend in the early twentieth century in South Africa (Hoffman et al., 2009), along with an increased frequency of drought and extreme events during the period subsequent to the late 1960s and into the 1980s (Fauchereau et al., 2003). The relatively sparse data available for such analyses should be noted. The problem of limited data is further compounded by high inter-annual climatic variability,

which is particularly characteristic of arid regions (Muller et al., 2008; Kane, 2009). Coefficients of variation in mean annual rainfall generally increase from east to west, exceeding 40% along the western margins of South Africa (Schulze, 1997). In such environments single storm events can make substantial contributions to the annual rainfall total (e.g. Muller et al., 2008). Cyclical temporal variability in rainfall has been identified at a range of frequencies, ranging from the (2–3 year) Quasi Biennial Oscillation (QBO) to a consistently identified 18 year variability cycle (Tyson, 1986; Mason and Jury, 1997). Summer-rainfall zone variability has been linked with the El Niño Southern Oscillation (ENSO; Lindesay, 1988; Washington and Todd, 1999; Rouault and Richard, 2003) with areas of NW/SE orientated lower level convergence, which are ordinarily responsible for considerable rainfall in the summer rainfall zone, shifting towards Madagascar and reducing summer rainfall during El Niño events (Washington and Todd, 1999). The most severe droughts in South Africa during the study period occurred in 1983 and 1992 (Rouault and Richard, 2003).

## 3. Methodology

### 3.1. Satellite vegetation index

We used 25 years (1982–2006) of GIMMS (Global Inventory Modelling and Mapping Studies) AVHRR-NDVI data for the initial determination of vegetation cover persistence across southern Africa because of the long record of this NDVI product (i.e. from 1982 to 2006 for the entire planet; Tucker et al., 2004). The GIMMS NDVI data have a nominal spatial resolution of 8 km and are provided every 16 days. The data were obtained from the Global Land Cover Facility ([www.landcover.org](http://www.landcover.org)) and are calibrated and corrected for variations in solar and view zenith angle, and the presence of stratospheric aerosols associated with the El Chichon and Mt Pinatubo volcanic eruptions (Tucker et al., 2005). Annual Maximum Value Composites (MVC) (Holben, 1986) were created and used as a surrogate value for the level of vegetation cover. To account for the timing of peak NDVI in the southern hemisphere, the annual MVC-NDVI composites were based on hydrological year, i.e. October to September as opposed to a calendar year. The hydrological year is designated by the calendar year in which it ends.

### 3.2. Ancillary data

Southern African biome data, based on the categorizations identified by Rutherford (1997), were made available in vector format by the South African National Biodiversity Institute (<http://www.plantzafrica.com>). The map contains 7 major biomes (Fig. 1). Monthly high resolution ( $0.5^\circ \times 0.5^\circ$ ) gridded precipitation data were also obtained from the University of East Anglia Climatic Research Unit dataset (CRU TS 3.0; Harris et al., 2013).

### 3.3. Persistence analysis

Spatial patterns of NDVI change were generated through an analysis of the persistence of NDVI trends (Lanfredi et al., 2004). An initial reference map was produced by constructing a linear NDVI trend surface  $s(x, y, t)$  over the reference period (1982–1991). Pixels  $(x, y)$  for which the trend sign was positive over this initial period ( $t = t_i$ ) were assigned a value of +1, otherwise a value of -1 was assigned. Using a yearly time step, NDVI values were then added and a new trend surface was created. If the addition of an additional year cleared an existing trend (i.e. the slope is set to zero), we assumed that the current status of the vegetation was statistically equivalent to the initial reference level (i.e. recovery). In practice, because of the noised nature of the NDVI

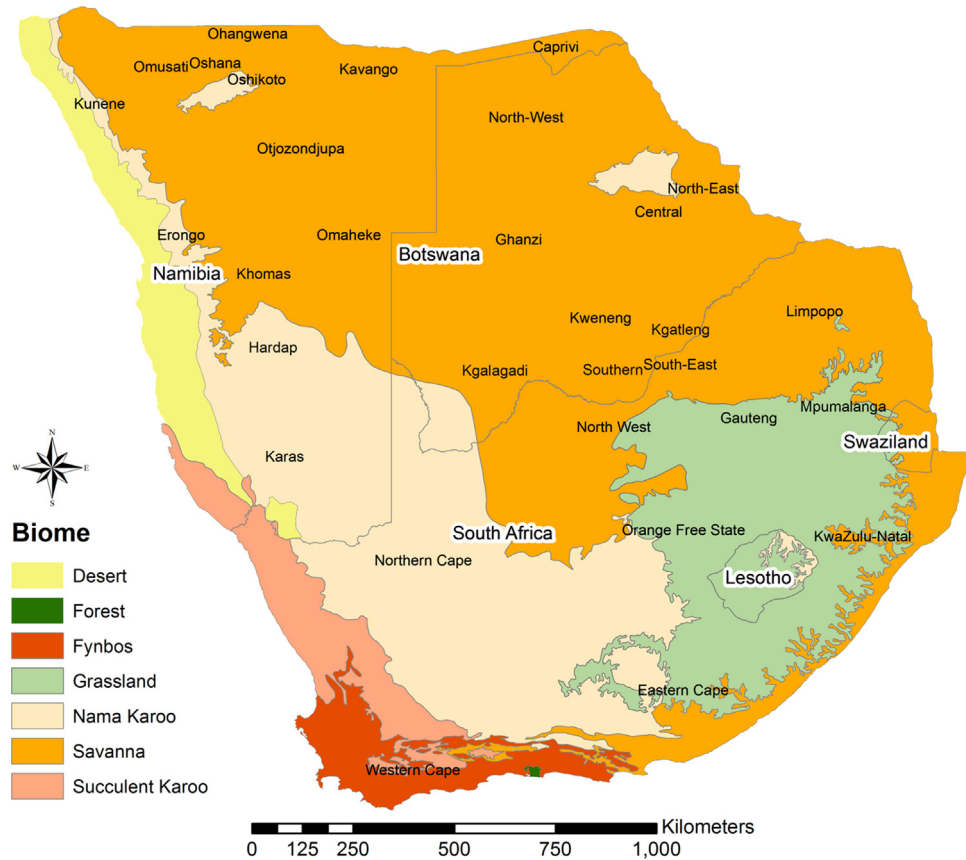


Fig. 1. The vegetation biomes of southern Africa according to Rutherford (1997).

time-series data, we cannot identify the exact point at which the slope of the trend returns to zero, but instead we detected the first passage time; when the NDVI field has just passed the return time and the trend has changed sign, i.e. positive to negative or vice versa (Simoniello et al., 2008 and Fig. 2). If the addition of a subsequent year was not sufficient to clear the previously estimated trend or to change its sign, the pixel was classified as persistent. The method focuses on identifying changes in NDVI trends as opposed to absolute values. This is important as, compared to other common methods of linear trend analyses, it limits the influence of the reference period on trend assessments (Wessels et al., 2012). Nevertheless, the reference period (1982–1991) was chosen to ensure, within the constraints of the available AVHRR data, that a wide range of climatic variability was incorporated.

Persistence maps  $P(x, y, t)$ , which kept track of persistent pixels, were constructed according to the rule:

$$P(x, y, t_i) = s(x, y, t_i) \quad t = t_i$$

$$P(x, y, t) \begin{cases} 0 & \text{if } s(x, y, t) \neq P(x, y, t-1) \\ P(x, y, t-1) & \text{if } s(x, y, t) = P(x, y, t-1) \end{cases} \quad t > t_i$$

A cumulative field  $P_{t_i}^T(x, y) = \sum_{t=t_i}^T P(x, y, t)$  was obtained at the observational time  $T$ , by adding all the persistence maps from  $t_i$  to  $T$ . For any pixel  $(x, y)$ , the magnitude of the field indicates the number of years during which inter-annual fluctuations have not been able to clear the trend (i.e. survival of the trend), and its sign indicates whether the tendency of the trend was positive or negative (Lanfredi et al., 2004). A positive persistence does not imply that NDVI values have progressively increased (or consistently decreased, in the case of negative persistence), for the duration of

the investigated period, just that the vegetation trend has not been cleared.

Persistence probability  $q(t)$  is defined as the probability that a given fluctuating field crosses a defined reference level within a chosen time interval  $t$ , before returning back to the reference level (Redner, 2001). The concept has been used for the characterisation of dynamic, spatially extended systems (e.g. Sire et al., 2000). It therefore represents an appropriate measure of resilience when using data of this nature (i.e. NDVI). We used the method of Lanfredi et al. (2004) to estimate persistence probabilities. For specific regions of interest, the distribution of the first passage time  $q(t)$  was estimated from the persistence maps (i.e. the proportion of non-cleared trends through time), using the equation:

$$q(t) = \frac{N(t)}{N(t_i)}$$

where  $N(t)$  and  $N(t_i)$  are the number of non-cleared trends having the same sign in  $P(x, y, t)$  and  $P(x, y, t_i)$ , respectively

An exponential decay law  $q(t) = e^{-t/\tau}$  was fitted to the surviving distribution of positive and negative trends to estimate the mean lifetime ( $\tau$ ) of a trend before it decays. Exponential decays have been shown to be particularly effective for characterising short memory stationary processes and have been used in a number of studies (Lanfredi et al., 2004; Simoniello et al., 2008; Coppola et al., 2009).

## 4. Results

### 4.1. Patterns of vegetation cover persistence

Fig. 3 shows the spatial and temporal patterns of trends in vegetation cover persistence across southern Africa for the period

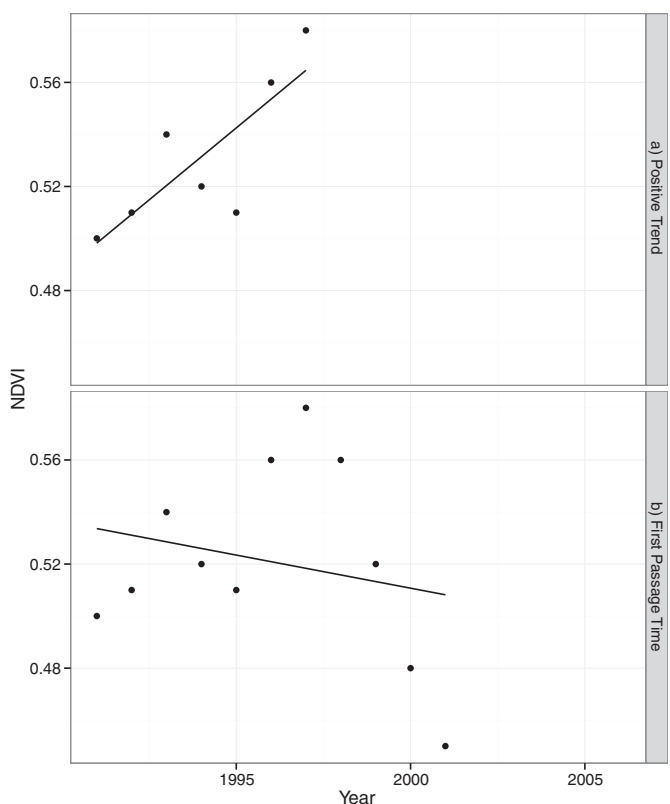


**Fig. 2.** A schematic diagram illustrating how trend signs are determined; (a) a linear trend is estimated over an initial reference period; and (b) additional years are added at yearly intervals, which modifies the slope of the trend until the trend changes sign; this is the first passage time.

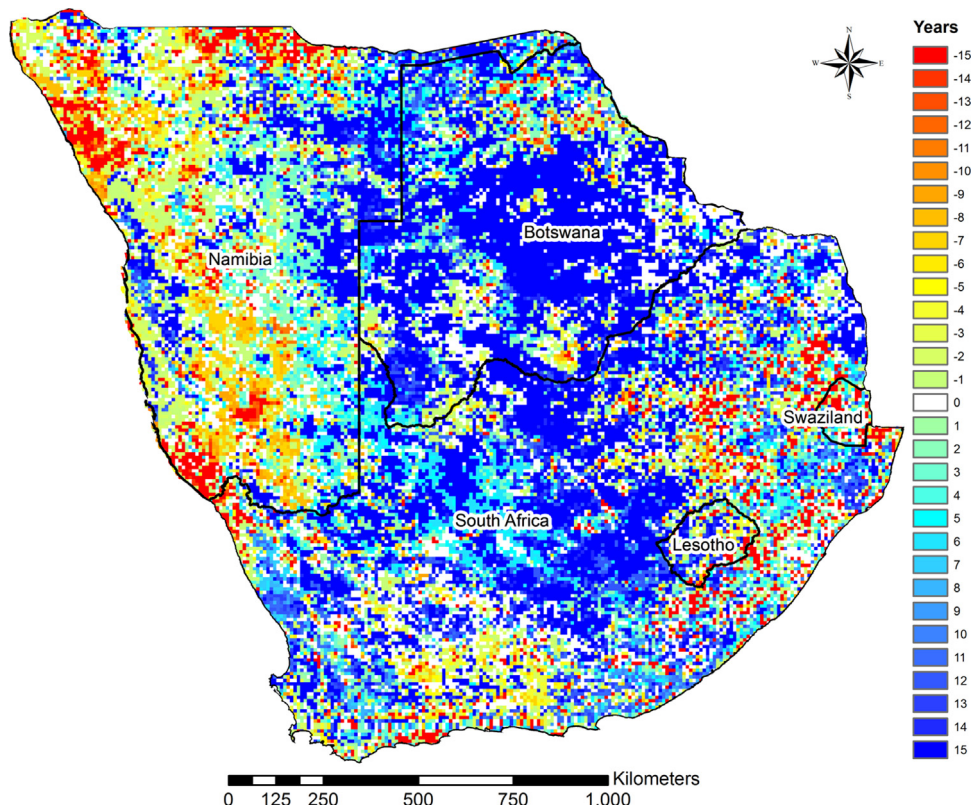


**Fig. 3.** Total persistence map of NDVI trends for the period 1991–2006 obtained from the 8 km GIMMS dataset. Persistence is expressed in number of years starting from 1991 and the sign of the trend is indicative of positive (+) or negative (-) trends. The period 1982–1991 is the reference period.

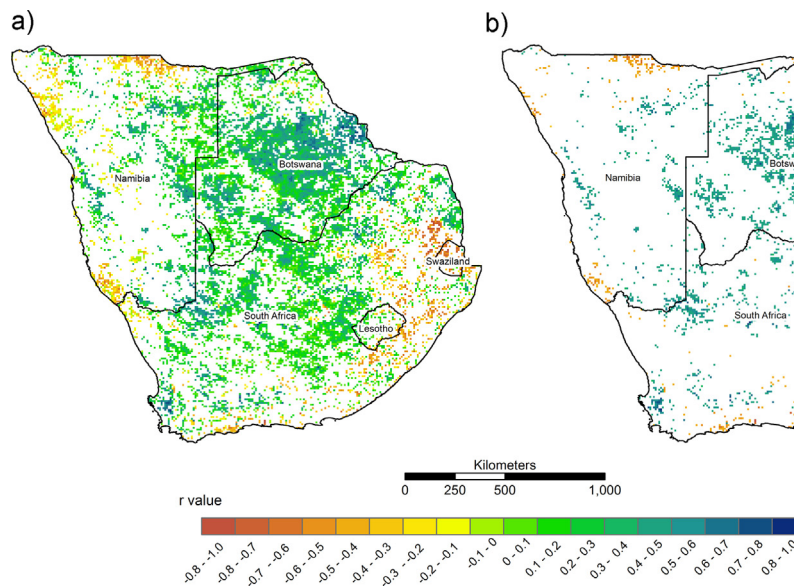


**Fig. 4.** Map of the correlation coefficient ( $r$ ) between NDVI and time over the period 1991–2006 for (a) all pixels characterised by  $|P_{1991}^{2006}(x,y)| = 16$ ; and (b) only pixels characterised by significant correlations ( $p < 0.05$ ).

1991–2006 (where 1991 is the end of the “reference period” and thus equates to year zero). The various blue shadings indicate areas where positive trends persist and the yellow to red shadings indicate areas where negative trends persist.

The patterns of persistence in both positive and negative NDVI trends show spatial coherence (Fig. 3). Positive trends dominate the landscape, with 57% of the total area characterised by positive NDVI trend persistence. Large clusters of positive trends can clearly be observed within the central parts of South Africa and Botswana. Conversely, negative trends are most apparent across western and northern portions of Namibia, eastern and southern South Africa and in Swaziland. Approximately one third of the pixels (34%) within the study area show evidence of long term persistence, i.e. a given trend has persisted for the entire 15 year period, whereas a further third (~34%) are characterised by trends that persist for 2 years or less (Fig. 3), indicating an initial reference period trend of low significance. Of the negative trends, 57% persisted for 2 years or less, compared to 22% of positive trends over the same time period, suggesting that overall, positive trends are more persistent.

Fig. 4 illustrates the strength of the correlation between NDVI and time, for trends characterised by maximum persistence over the study period (i.e. trends that have persisted for 15 years). Approximately 8% of the pixels within the study area are characterised by maximum persistence (i.e. 15 years) and show a significant ( $p < 0.05$ ) correlation between NDVI and time. Significant persistent positive trends were most prominent (Fig. 4b). The largest persistent positive trend clusters can be seen across the Savanna region of central and eastern Botswana. In contrast, along the Kavango River in northern Namibia, central and northern Swaziland, large parts of South Africa east of Johannesburg, and parts of KwaZulu-Natal along the steep slopes of the Drakensburg Escarpment, are characterised by significant negative persistent trends.

Pixels characterised by persistent trends of low significance ( $p > 0.05$ ) cover approximately 26% of the study area (Fig. 4). These pixels are indicative of a fluctuating inter-annual NDVI values, which cause noise within the data, but over the entire time-series a weak trend remains consistent (positive or negative). This phenomena is most pronounced in regions where vegetation is sparse or absent, such as regions of western Namibia where negative vegetation persistence is high but the correlation between

**Table 1**

Percentage of pixels exhibiting positive and negative trends during the reference period (1982–1991) and mean lifetimes  $\tau$  for each biome.

Biome	Positive trends		Negative trends	
	%	$\tau$ (years)	%	$\tau$ (years)
Savanna	67	26.3	33	8.6
Nama-Karoo	68	17.5	32	5.7
Fynbos	61	13	39	10.8
Grassland	62	16.9	38	15.6
Succulent Karoo	72	9.9	28	12.5

NDVI and time is weak and not significant ( $p > 0.05$ ; Fig. 4a). In such regions, NDVI values are low (data not shown) and their fluctuation may be more indicative of short-term changes in the moisture content of the exposed surface rather than significant changes in vegetation cover or vitality.

#### 4.2. Characteristic decay time of NDVI trends

Biome resilience was estimated by considering the persistence probability of positive and negative trends. From this, the characteristic decay times for positive and negative trends were analysed and exponential fits were used to estimate the mean lifetime of trends. The resulting plots of persistence probability (Fig. 5) illustrate the exponential nature of the relationship between persistence probability and time. Temporal deviations can be seen in the rate of trend extinction for the Nama and Succulent Karoo biomes. For instance, the plot for the Nama Karoo shows a rapid decrease in positive persistence probability in 1997 and 1998. In contrast, during the same time period the persistence probability of negative trends remains stable, and instead drops rapidly in 1999 (Fig. 5b).

Within all biomes, the number of pixels exhibiting a positive trend in NDVI is greater than those with a negative trend. This can be represented numerically as the mean lifetime for the survival of any trend (Table 1). The Savanna and Nama-Karoo biomes have the highest percentage of positive trend pixels (67% and 68%; respectively) and are both characterised by a marked asymmetry between the mean lifetime of positive and negative trends (Table 1 and Fig. 5). That is, in both biomes, negative trends decay faster than

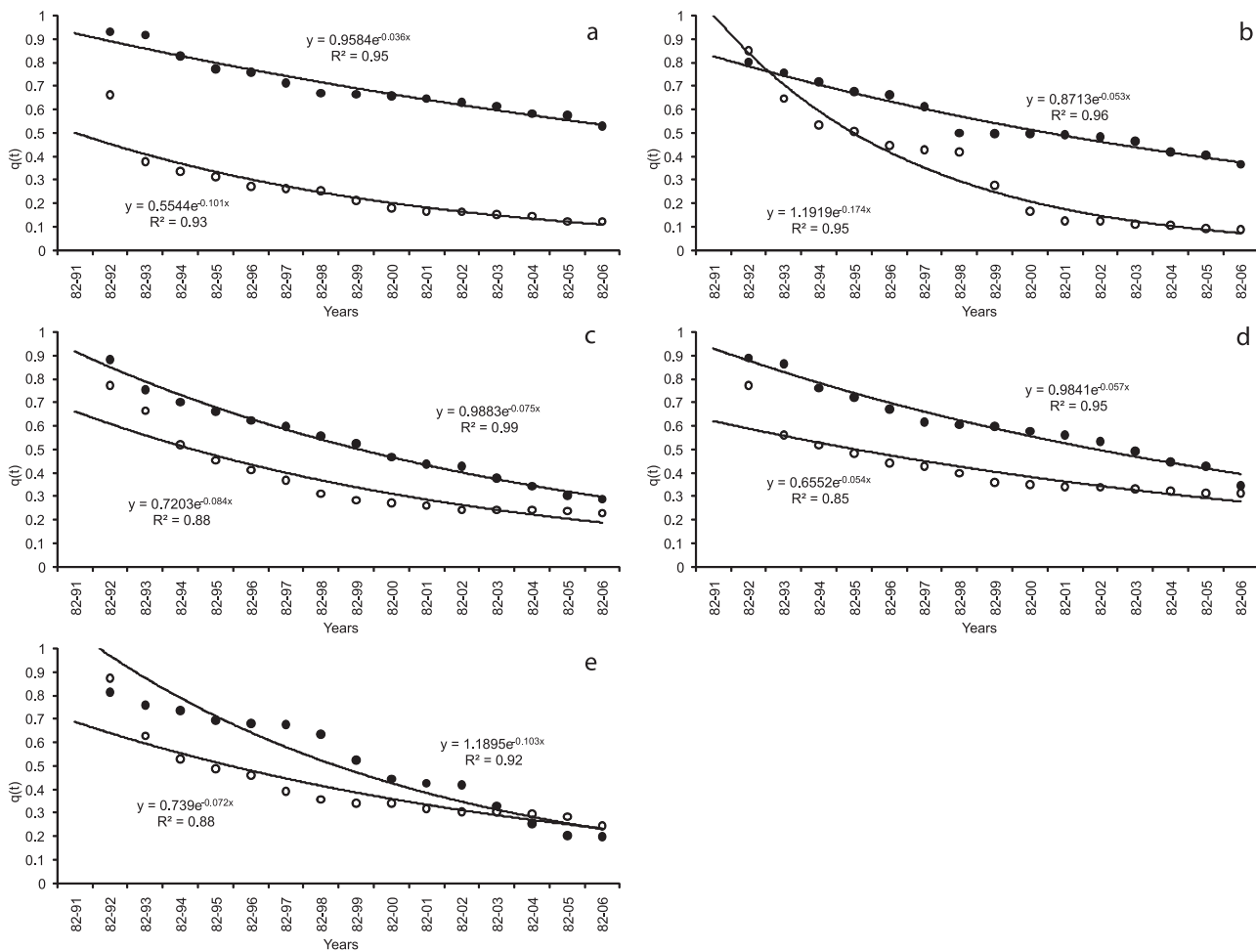


**Fig. 5.** Persistence probability ( $q(t)$ ) plots of positive (●) and negative (○) trends obtained by fitting an exponential decay law for (a) Savanna, (b) Nama Karoo, (c) Fynbos, (d) Grassland and (e) Succulent Karoo biomes.

the positive trends. The mean lifetime of negative trends is shortest in the Nama Karoo and the mean lifetime of positive trends in the Savanna biome is the longest of all biomes examined (Table 1). In contrast the mean lifetimes for positive and negative trends are very similar within the Fynbos and Grassland biomes. Of all the biomes examined, the Succulent Karoo region has the greatest proportion of positive trend pixels, but has the shortest mean lifetime for positive trends and second longest mean lifetime for negative trend survival (Table 1).

## 5. Discussion

At the regional-scale, the dominance of observed positive NDVI trend persistence paints an optimistic picture. The observed spatial patterns of predominantly persistent positive NDVI trends across central parts of South Africa and Botswana and negative trend persistence across western and northern portions of Namibia are similar to the recent observations of Fensholt et al. (2012), who used the AVHRR-GIMMS dataset to analyse global trends in vegetation greenness in semi-arid regions. Furthermore, in the present study several areas characterised by persistent negative trends are either located in highly populated regions, such as the Kavango River in northern Namibia (Kgathi et al., 2006), and/or located close to urbanised areas, such as to the area east of Johannesburg. Additionally, negative trends can be associated with areas previously reported to be suffering from land degradation, such as central and northern Swaziland (Stringer et al., 2009), inland and

central KwaZulu-Natal and the Eastern Cape of South Africa (Hoffman and Todd, 2000). Such studies are largely based upon in situ data collection and participatory research approaches. Over 60% of the significant negative trends observed in South Africa, Swaziland and Lesotho, are also in regions where the ecosystem status has been previously identified as vulnerable (36%), endangered (23%) or critically endangered (23%) (South African National Biodiversity Institute, 2004). The area of strong positive persistence north of Cape Town is probably the result of agriculture on the formerly Renosterveld vegetation of the Swartland and perhaps viticulture in the Olifants River area.

Persistence probabilities were estimated in order to assess resilience within individual biomes. Temporal deviations in the probability plots observed for the two Karoo biomes, such as the rapid decreases in the persistence probabilities of positive trends in 1997 and 1998 and negative trends in 1999 (Fig. 5b), may be a consequence of the vegetative response to climatic oscillations, i.e. El Niño and La Niña, which are seen in precipitation anomaly data (Fig. 6a). The precipitation data show the presence of drier than average conditions in the years 1997 and 1998, which coincide with an El Niño event, and conversely substantially wetter than average conditions during 1999 and 2000, coincident with La Niña. A similar correspondence between the rate of trend extinction and precipitation can be observed for the Succulent Karoo (Figs. 5e and 6b). Here the level of precipitation remains below average from 1997 to 1999, which results in the more rapid extinction (than the fitted data) of positive trends between 1997 and 2000

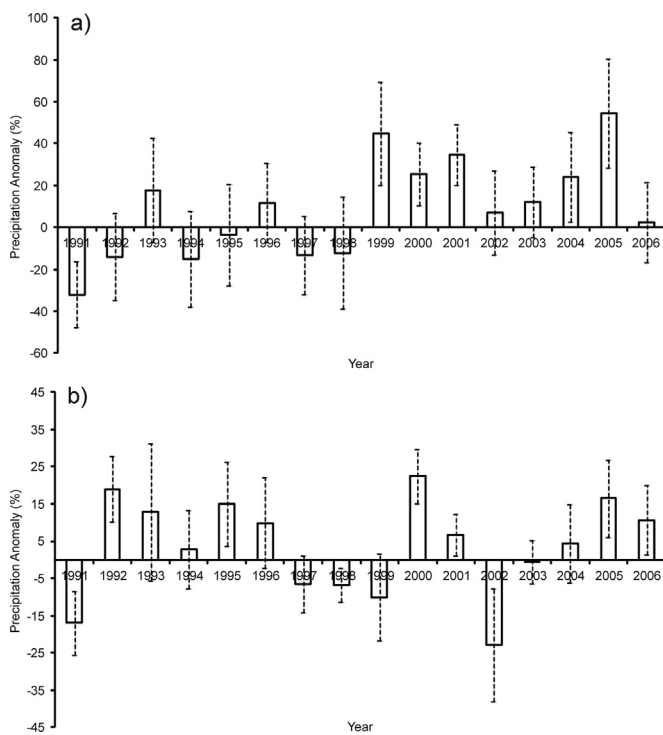


**Fig. 6.** Spatially aggregated precipitation anomalies derived from the CRU TS 3.0 gridded dataset for (a) the Nama Karoo and (b) the Succulent Karoo biomes. The time period 1982–1991 is taken as the reference period, against which yearly anomalies are obtained. Error bars indicate  $\pm 1$  sd.

(Fig. 5e). The correspondence in the timing of the observed trend extinctions in relation to precipitation patterns, particularly those influenced by ENSO oscillations, can be related to previous studies that have shown a close correspondence between satellite-derived vegetation greenness and precipitation in similar regions (Fensholt et al., 2012; Hickler et al., 2005; Hellden and Ottrup, 2008; Huber et al., 2011). Our biome-scale results also correspond with those of Wiegand and Milton (1996) who simulated the dynamics of Karoo shrubland and found that short-term vegetation dynamics were sensitive to rainfall pattern.

The estimated mean lifetimes of trend persistence suggest that vegetation resilience is lowest in the Succulent Karoo. The potential climatically driven positive trend extinctions observed in the Succulent Karoo persistence probability plot (Figs. 5 and 6) may account for the short mean lifetime of positive trends in this biome, whereas the comparatively long lifetime for negative trend survival is likely to be a consequence of a slow rate of vegetation recovery, which is a characteristic of semi-arid shrub ecosystems (Wiegand et al., 1995). While the specific responses of individual plant genera and species to drought stress are poorly understood for the Succulent Karoo (e.g. Hoffman et al., 2009, and references therein), a strong correlation between NDVI and rainfall variables (mean annual precipitation (MAP), coefficient of variation of MAP and potential evapotranspiration (PET)) have been reported for the winter rainfall Succulent Karoo (e.g. Fox et al., 2005). Similar mean lifetimes for both negative and positive trends were observed in the Fynbos and Grassland biomes and are difficult to interpret because both biomes are characterised by a substantial coverage of agricultural, urbanised or managed land, where vegetation responds to both natural environmental variability, but also to anthropic manipulation.

Our results could be interpreted as showing that the Savanna and Nama Karoo biomes show signs of strong vegetation resilience. However, while patterns of positive NDVI trend persistence might

be interpreted as indicative of “healthy” vegetation (Lanfredi et al., 2004), in the context of the present study and many other semi-arid environments, such patterns cannot be assumed to represent a “positive” ecological outcome. This reflects some of the fundamental difficulties associated with interpreting the NDVI, which is a generic ecosystem measure. For example, it cannot identify changes in species or plant functional type. Thus, an increase in the density of woody plants in a Savanna may appear as a positive persistent trend even though such bush encroachment is usually considered detrimental to both ecological diversity and livestock carrying capacity (Scholes and Archer, 1997). Similarly, in the context of land degradation, changing graze or forage quality cannot be detected (Wessels et al., 2007a). Therefore, as with all satellite-based vegetation trend analyses, caution must be taken when interpreting the outputs without reference to in situ field data. A current lack of available field data at the appropriate spatial and temporal resolution prevents a direct quantitative evaluation of the method and persistence trends presented within this study. This is a common limitation of vegetation index trend analyses at this scale (Wessels et al., 2012). However, a qualitative comparison of our results with other studies helps to place confidence in our approach. Further work is required to provide a detailed interpretation, particularly in specific regions or locations. For example, several studies have sought to use satellite-derived measures of greenness to specifically monitor human-induced land degradation by removing the rainfall signal from the NDVI trend signal (e.g. RESTREND method; Wessels et al., 2007b). Further work could establish the utility of using such an approach to extend the current analyses in order to identify areas that may be affected by anthropogenic-induced change of the land surface.

The observed vegetation persistence patterns should also be interpreted with reference to the spatial and temporal scale of observation. Our results suggest that at the spatial scale of this investigation (8 km pixels), climatic patterns and the ENSO oscillation in particular, may influence temporal patterns in vegetation activity. The spatial resolution of the data is therefore appropriate for global and regional land surface modelling, where characteristic timescales of vegetation persistence and recovery may be used to test model performance or be utilised within a multi-scale analysis framework where coarse resolution data are used to identify sites of interest for higher resolution analysis. Whilst the temporal extent of the dataset (i.e. 25 years) has an influence of the estimated time-scales of vegetation cover recovery and thus resilience, the exponential nature of the biome persistence probability plots suggest that the temporal extent of the study is sufficiently long to capture vegetation cover responses to environmental perturbations, thus allowing comparisons of resilience between biomes to be made. Despite its limitations, remote sensing is often the only way of obtaining spatially continuous data of this nature across large spatial extents.

## 6. Conclusions

The aim of this study was to use remotely sensed data to characterise spatial and temporal patterns of vegetation dynamics and resilience across southern Africa. Results obtained at the continent scale show a preponderance of positive NDVI trends, covering 57% of the landscape. Persistent negative NDVI trends were also identified across the landscape, the locations of which often matched well with areas known to be affected by human disturbance (e.g. Northern Namibia, parts of KwaZulu-Natal and Swaziland) and/or areas where the ecosystem status has been previously identified as of concern (e.g. South African National Biodiversity Institute, 2004).

More detailed analyses of persistence probability plots and characteristic decay times of NDVI trends were undertaken at the biome

level. Persistence properties of vegetation at the biome scale are likely a reflection of the growth forms or plant functional types that characterise particular biomes, more specifically, their response(s) to mortality events and recruitment strategies during recovery periods. The results of this study highlight differences in the persistence characteristics of the vegetation cover between biomes. In the Savanna and Nama Karoo, mean lifetimes for positive NDVI trends are much longer than those of negative trends. In contrast, in the Succulent Karoo long mean lifetimes for negative NDVI trends, in comparison to positive trends, suggest that vegetation is much less resilient. In this instance, at the scale of this study, it was also possible to link the rate of positive trend extinctions with climatically driven phenomena.

The study has provided an insight into how remotely sensed data may be used to estimate biome-specific time-scales of vegetation persistent behaviour. When linked appropriately with climatic and anthropic drivers of environmental disturbance, the results could ultimately provide insights into the complex interactions between land cover, environment, climate and human activity. These data can also be used to identify areas of potential vulnerability, which may require a more detailed investigation and can be related to more specific localised phenomena, such as land cover and land use change.

## References

- Beck, H.E., McVicar, T.R., van Dijk, A.I.J.M., Schellekens, J., de Jeu, R.A.M., Bruijnzeel, L.A., 2011. Global evaluation of four AVHRR-NDVI data sets: intercomparison and assessment against Landsat imagery. *Remote Sens. Environ.* 115, 2547–2563.
- Coppola, R., Cuomo, V., D'Emilio, M., Lanfredi, M., Liberti, M., Macchiato, M., Simoniello, T., 2009. Terrestrial vegetation cover activity as a problem of fluctuating surfaces. *Int. J. Mod. Phys. B* 23, 5444–5452.
- de Jong, R., de Bruin, S., de Wit, A., Schaepman, M.E., Dent, D.L., 2011. Analysis of monotonic greening and browning trends from global NDVI time-series. *Remote Sens. Environ.* 115, 692–702.
- Dlamini, W.M., 2011. Bioclimatic modeling of southern African bioregions and biomes using Bayesian networks. *Ecosystems* 14, 366–381.
- Fauchereau, N., Trzaska, S., Rouault, M., Richard, Y., 2003. Rainfall variability and changes in southern Africa during the 20th century in the global warming context. *Nat. Hazards* 29, 139–154.
- Fensholt, R., Langanke, T., Rasmussen, K., Reenberg, A., Prince, S.D., Tucker, C., Scholes, R.J., Le, Q.B., Bondeau, A., Eastman, R., Epstein, H., Gaughan, A.E., Hellden, U., Mbow, C., Olsson, L., Paruelo, J., Schweitzer, C., Seaquist, J., Wessels, K., 2012. Greenness in semi-arid areas across the globe 1981–2007—an Earth Observing Satellite based analysis of trends and drivers. *Remote Sens. Environ.* 121, 144–158.
- Fox, S.C., Hoffman, M.T., Hoare, D., 2005. The phenological pattern of vegetation in Namaqualand, South Africa and its climatic correlates using NOAA-AVHRR NDVI data. *S. Afr. Geogr. J.* 87, 85–94.
- Gunderson, L.H., 2000. Ecological resilience—in theory and application. *Annu. Rev. Ecol. Syst.* 31, 425–439.
- Harris, I., Jones, P.D., Osborn, T.J., Lister, D.H., 2013. Updated high-resolution grids of monthly climatic observations—the CRU TS 3.10 data set. *Int. J. Climatol.*, <http://dx.doi.org/10.1002/joc.3711>.
- Hellden, U., Ottupur, C., 2008. Regional desertification: a global synthesis. *Global Planet. Change* 64, 169–176.
- Hickler, T., Eklundh, L., Seaquist, J.W., Smith, B., Ardo, J., Olsson, L., Sykes, M.T., Sjostrom, M., 2005. Precipitation controls Sahel greening trend. *Geophys. Res. Lett.* 3, 2, <http://dx.doi.org/10.1029/2005GL024370>.
- Hoffman, M.T., Carrick, P.J., Gillson, L., West, A.G., 2009. Drought, climate change and vegetation response in the Succulent Karoo, South Africa. *S. Afr. J. Sci.* 105, 54–60.
- Hoffman, M.T., Todd, S., 2000. A national review of land degradation in South Africa: the influence of biophysical and socio-economic factors. *J. S. Afr. Stud.* 26, 743–758.
- Holben, B.N., 1986. Characteristics of maximum-value composite images from temporal AVHRR data. *Int. J. Remote Sens.* 7, 1417–1434.
- Holling, C.S., 1996. Engineering Resilience versus Ecological Resilience. *Engineering Within Ecological Constraints*, PC, Schulze. National Academy Press, Washington, DC, pp. 31–43.
- Huber, S., Fensholt, R., 2011. Analysis of teleconnections between AVHRR-based sea surface temperature and vegetation productivity in the semi-arid Sahel. *Remote Sens. Environ.* 115, 3276–3285.
- Huber, S., Fensholt, R., Rasmussen, K., 2011. Water availability as the driver of vegetation dynamics in the African Sahel from 1982 to 2007. *Global Planet. Change* 76, 186–195.
- Hutyra, L.R., Munger, J.W., Nobre, C.A., Saleska, S.R., Vieira, S.A., Wofsy, S.C., 2005. Climatic variability and vegetation vulnerability in Amazonia. *Geophys. Res. Lett.* 32, 2–5.
- IPCC, 2007. In: Solomon, S., Qin, D., Manning, M., Chen, Z., Marquis, M., Averyt, K.B., Tignor, M., Miller, H.L. (Eds.), *Climate Change 2007: The Physical Science Basis. Contribution of Working Group I to the Fourth Assessment Report of the Intergovernmental Panel on Climate Change*. Cambridge, UK and New York, USA, p. 996.
- Ives, A.R., 1995. Measuring resilience in stochastic-systems. *Ecol. Mono* 65, 217–233.
- Kane, R.P., 2009. Periodicities, ENSO effects and trends of some South African rainfall series: an update. *S. Afr. J. Sci.* 105, 199–207.
- Kgathi, D.L., Kniveton, D., Ringrose, S., Turton, A.R., Vanderpost, C.H.M., Lundqvist, J., Seely, M., 2006. The Okavango: a river supporting its people, environment and economic development. *J. Hydrol.* 331, 3–17.
- Lanfredi, M., Simoniello, T., Macchiato, M., 2004. Temporal persistence in vegetation cover changes observed from satellite: development of an estimation procedure in the test site of the Mediterranean Italy. *Remote Sen. Environ.* 93, 565–576.
- Lindesay, J.A., 1988. South-African rainfall, the Southern Oscillation and a southern-hemisphere semi-annual cycle. *J. Climatol.* 8, 17–30.
- Lindesay, J.A., 1998. The present climates of southern Africa. In: Hobbs, J.E., Lindesay, J.A., Bridgeman, H.A. (Eds.), *Climates of the Southern Continents: Present, Past and Future*. Wiley, Chichester, pp. 5–52.
- Mason, S.J., Jury, M.R., 1997. Climatic variability and change over southern Africa: a reflection on underlying processes. *Prog. Phys. Geogr.* 21, 23–50.
- Midgley, G.F., Thuiller, W., 2011. Potential responses of terrestrial biodiversity in southern Africa to anthropogenic climate change. *Reg. Environ. Change* 11, S127–S135.
- Mittelbach, G.G., Turner, A.M., Hall, D.J., Rettig, J.E., Osenberg, C.W., 1995. Perturbation and resilience—a long-term, whole-lake study of predator extinction and reintroduction. *Ecology* 76, 2347–2360.
- Muller, A., Reason, C.J.C., Fauchereau, N., 2008. Extreme rainfall in the Namib Desert during late summer 2006 and influences of regional ocean variability. *Int. J. Climatol.* 28, 1061–1070.
- Myneni, R.B., Nemani, R.R., Running, S.W., 1997. Estimation of global leaf area index and absorbed par using radiative transfer models. *IEEE Trans. Geosci. Remote* 35, 1380–1393.
- Nemani, R.R., Keeling, C.D., Hashimoto, H., Jolly, W.M., Piper, S.C., Tucker, C.J., Myneni, R.B., Running, S.W., 2003. Climate-driven increases in global terrestrial net primary production from 1982 to 1999. *Science* 300, 1560–1563.
- Redner, S., 2001. *A Guide to First Passage Processes*. Cambridge University Press, Cambridge, UK.
- Reynolds, J.F., Smith, D.M.S., Lambin, E.F., Turner, B.L., Mortimore, I.I., Batterbury, M., Downing, S.P., Dowlatabadi, T.E., Fernandez, H., Herrick, R.J., Huber-Sannwald, J.E., Jiang, E., Leemans, H., Lynam, R., Maestre, T., Ayarza, F.T., Walker, M.B., 2007. Global desertification: building a science for dryland development. *Science* 316, 847–851.
- Richard, Y., Fauchereau, N., Poccard, I., Rouault, M., Trzaska, S., 2001. 20th century droughts in southern Africa: spatial and temporal variability, teleconnections with oceanic and atmospheric conditions. *Int. J. Climatol.* 21, 873–885.
- Rouault, M., Richard, Y., 2003. Intensity and spatial extension of drought in South Africa at different time scales. *Water SA* 29, 489–500.
- Rutherford, M.C., 1997. *Categorization of Biomes*. Cambridge University Press, New York, USA.
- Schapoff, S., Lucht, W., Gerten, D., Sitch, S., Cramer, W., Prentice, I.C., 2006. Terrestrial biosphere carbon storage under alternative climate projections. *Climatic Change* 74, 97–122.
- Scholes, R.J., Archer, S.R., 1997. Tree–grass interactions in savannas. *Annu. Rev. Ecol. Syst.* 28, 517–544.
- Scholze, M., Knorr, W., Arnell, N.W., Prentice, I.C., 2006. A climate-change risk analysis for world ecosystems. *Proc. Natl. Acad. Sci. U.S.A.* 103, 13116–13120.
- Schulze, R.E., 1997. Impacts of global climate change in a hydrologically vulnerable region: challenges to South African hydrologists. *Prog. Phys. Geogr.* 21, 113–136.
- Simoniello, T., Lanfredi, M., Liberti, M., Coppola, R., Macchiato, M., 2008. Estimation of vegetation cover resilience from satellite time series. *Hydrol. Earth Syst. Sci.* 12, 1053–1064.
- Sire, C., Majumdar, S.N., Rudinger, A., 2000. Analytical results for random walk persistence. *Phys. Rev. E* 61, 1258–1269.
- Stringer, L.C., Dyer, J.C., Reed, M.S., Dougill, A.J., Twyman, C., Mkwambisi, D., 2009. Adaptations to climate change, drought and desertification: local insights to enhance policy in southern Africa. *Environ. Sci. Policy* 12, 748–765.
- Thomas, D.S.G., Knight, M., Wiggs, G.F.S., 2005. Remobilization of southern African desert dune systems by twenty-first century global warming. *Nature* 435, 1218–1221.
- Tilman, D., Downing, J.A., 1994. Biodiversity and stability in grasslands. *Nature* 367, 363–365.
- Tucker, C.J., 1979. Red and photographic infrared linear combinations for monitoring vegetation. *Remote Sens. Environ.* 8, 127–150.
- Tucker, C.J., Pinzon, J.E., Brown, M.E., 2004. Global Inventory Modeling and Mapping Studies, Global Land Cover Facility. University of Maryland, College Park, Maryland.
- Tucker, C.J., Pinzon, J.E., Brown, M.E., Slayback, D.A., Pak, E.W., Mahoney, R., Vermote, E.F., El Saleous, N., 2005. An extended AVHRR 8-km NDVI dataset compatible with MODIS and SPOT vegetation NDVI data. *Int. J. Remote Sens.* 26, 4485–4498.
- Tyson, P.D., 1986. *Climatic Change and Variability in Southern Africa*. Oxford University Press, Cape Town.

- Washington, R., Todd, M., 1999. Tropical-temperate links in southern African and Southwest Indian Ocean satellite-derived daily rainfall. *Int. J. Climatol.* 19, 1601–1616.
- Wessels, K., Steenkamp, K., von Maltitz, G., Archibald, S., 2011. Remotely sensed vegetation phenology for describing and predicting the biomes of South Africa. *Appl. Veg. Sci.* 14, 49–66.
- Wessels, K.J., Bergh, F.v.d., Scholed, R.J., 2012. Limits to detectability of land degradation by trend analysis of vegetation index data. *Remote Sen. Environ.* 125, 10–22.
- Wessels, K.J., Prince, S.D., Carroll, M., Malherbe, J., 2007a. Relevance of rangeland and degradation in semiarid northeastern South Africa to the nonequilibrium theory. *Ecol. Appl.* 17, 815–827.
- Wessels, K.J., Prince, S.D., Malherbe, J., Small, J., Frost, P.E., VanZyl, D., 2007b. Can human-induced land degradation be distinguished from the effects of rainfall variability? A case study in South Africa. *J. Arid Environ.* 68, 271–297.
- Wiegand, T., Milton, S.J., 1996. Vegetation change in semiarid communities—simulating probabilities and time scales. *Vegetation* 125, 169–183.
- Wiegand, T., Milton, S.J., Wissel, C., 1995. A simulation-model for a shrub ecosystem in the semiarid Karoo, South-Africa. *Ecology* 76, 2205–2221.
- Wissel, C., 1984. A universal law of the characteristic return time near thresholds. *Oecologia* 65, 101–107.
- Xiao, J., Moody, A., 2005. A comparison of methods for estimating fractional green vegetation cover within a desert-to-upland transition zone in central New Mexico, USA. *Remote Sen. Environ.* 98, 237–250.